

# Research progress on vanadium oxides for potassium-ion batteries

Yuhan Wu<sup>1, †</sup>, Guangbo Chen<sup>2</sup>, Xiaonan Wu<sup>3</sup>, Lin Li<sup>4</sup>, Jinyu Yue<sup>1</sup>, Yinyan Guan<sup>1, †</sup>, Juan Hou<sup>5, †</sup>, Fanian Shi<sup>1, †</sup>, and Jiyan Liang<sup>1</sup>

<sup>1</sup>School of Environmental and Chemical Engineering, Shenyang University of Technology, Shenyang 110870, China

<sup>2</sup>Center for Advancing Electronics Dresden (cfaed), Department of Chemistry and Food Chemistry, Technische Universität Dresden, Dresden 01062, Germany

<sup>3</sup>Department of Chemical Engineering, Hebei Petroleum University of Technology, Chengde 067000, China

<sup>4</sup>Institute for Carbon Neutralization, College of Chemistry and Materials Engineering, Wenzhou University, Wenzhou 325035, China

<sup>5</sup>College of Science/Key Laboratory of Ecophysics and Department of Physics, Shihezi University, Shihezi 832003, China

**Abstract:** Potassium-ion batteries (PIBs) have been considered as promising candidates in the post-lithium-ion battery era. Till now, a large number of materials have been used as electrode materials for PIBs, among which vanadium oxides exhibit great potentiality. Vanadium oxides can provide multiple electron transfers during electrochemical reactions because vanadium possesses a variety of oxidation states. Meanwhile, their relatively low cost and superior material, structural, and physicochemical properties endow them with strong competitiveness. Although some inspiring research results have been achieved, many issues and challenges remain to be further addressed. Herein, we systematically summarize the research progress of vanadium oxides for PIBs. Then, feasible improvement strategies for the material properties and electrochemical performance are introduced. Finally, the existing challenges and perspectives are discussed with a view to promoting the development of vanadium oxides and accelerating their practical applications.

**Key words:** potassium-ion batteries; vanadium oxides; electrode materials; electrochemical performance; improvement strategies

**Citation:** Y H Wu, G B Chen, X N Wu, L Li, J Y Yue, Y Y Guan, J Hou, F N Shi, and J Y Liang, Research progress on vanadium oxides for potassium-ion batteries[J]. *J. Semicond.*, 2023, 44(4), 041701. <https://doi.org/10.1088/1674-4926/44/4/041701>

## 1. Introduction

In the twenty-first century, the increasing growth of fossil fuel consumption has caused a global energy crisis and environmental pollution, which limits the further development of human society to a large extent. Fortunately, natural renewable energy sources, such as sunlight, wind, tides, and hydro-power provide novel possibilities to replace fossil fuels. Nonetheless, these energy sources usually cannot be used directly and are not available timely. They are greatly affected by the factor of climate, season, and geography. To realize their high-efficient utilization, a feasible strategy is to convert them into electrical energy. The converted electrical energy can easily be stored by electrochemical energy storage technologies and can be used at any time<sup>[1–11]</sup>.

In the past few decades, lithium-ion batteries (LIBs) as the most successful electrochemical energy storage technology have been widely applied since they were commercialized by the Sony Company. Compared with other commercial batteries, LIBs possess the advantages of long-term cycle life, high energy densities, and environmental benignity. Re-

cently, the rapid development of electric vehicles has promoted the mass production of LIBs, resulting in a large consumption of Li resources. It is estimated that LIBs will consume 65% of total consumption by 2025<sup>[12]</sup>. However, rare Li resources will be unable to meet such high demand. According to the consumption rate projected for 2050, the Li reserve on land will be depleted around 2080<sup>[12]</sup>. In addition, the majority of the Li resource (~70%) are stored in South America, which seriously threatens the safe supply and price stability of Li<sup>[13]</sup>. In this case, novel batteries have been developed successively to serve as alternatives or supplements to LIBs, such as sodium-, zinc-, and magnesium-ion batteries. Among them, potassium-ion batteries (PIBs) are highly competitive. For example, Li<sup>+</sup> and K<sup>+</sup> belong to the family of alkali metal ions and show similar electrochemical behaviors in ion batteries (Table 1). The redox potential of K<sup>+</sup>/K [−2.93 V vs. standard hydrogen electrode (SHE)] is very close to that of Li<sup>+</sup>/Li (−3.04 V vs. SHE), indicating that PIBs and LIBs have similar energy densities theoretically. In addition, a low-cost advantage endows PIBs with competitiveness. K is widespread because its resource is as high as 17 000 ppm in Earth's crust, while the Li resource is only 20 ppm. It is also widely and evenly distributed in the Earth's crust. Unlike the alloy reaction between aluminum and Li at low voltage ranges, K does not form any intermetallic compounds with aluminum. Therefore, cheaper and lighter aluminum foil can be used as an anode current collector in PIBs, which reduces the cost and in-

Correspondence to: Y H Wu, [yuhanwu@sut.edu.cn](mailto:yuhanwu@sut.edu.cn); Y Y Guan, [guanyinyan@sut.edu.cn](mailto:guanyinyan@sut.edu.cn); J Hou, [hjuan05@sina.com](mailto:hjuan05@sina.com); F N Shi, [shifn@sut.edu.cn](mailto:shifn@sut.edu.cn)

Received 1 NOVEMBER 2022; Revised 14 NOVEMBER 2022.

©2023 Chinese Institute of Electronics

Table 1. Property comparison of K with Li<sup>[19–21]</sup>.

Parameter	Li	K
Atomic number	3	19
Atomic mass (g/mol)	6.94	39.10
$E^0$ versus SHE (V)	−3.04	−2.93
Melting point (°C)	180.5	63.5
Ionic radius (Å)	0.76	1.38
Stokes radius in water (Å)	2.38	1.25
Stokes radius in PC (Å)	4.8	3.6
Ionic conductivity in PC (S-cm <sup>2</sup> /mol)	8.3	15.2
Desolvation energy in PC (kJ/mol)	215.8	119.2
Abundance in Earth's crust (ppm)	20	17,000
Globe distribution	Mainly in South America	Many countries
Alloy with aluminum	Yes	No
Price of carbonate (US \$/kg)	356	121
Price of carbonate (US \$/Mole)	26.3	14.1

creases the energy density. In comparison to that of Li<sub>2</sub>CO<sub>3</sub> (≥99.0% purity), the price of K<sub>2</sub>CO<sub>3</sub> (≥99.0% purity) is much lower<sup>[14]</sup>. Additionally, K<sup>+</sup> has better transport properties potentially, which is in favor of rate performance. Despite the larger ionic radius of K<sup>+</sup>, its Stokes radii in various solvents are smaller because of its weaker Lewis acidity. The higher ionic conductivity and lower desolvation energy of K<sup>+</sup> also contribute to electrochemical reaction kinetics<sup>[15–18]</sup>. Furthermore, metal dendrites derived safety problem can be effectively relieved due to the low melting point of K (63.5 °C). K dendrites can be melted by Joule heat when metal plating leads to internal short circuits at overcharged states.

Electrode materials (including cathode and anode materials) play decisive roles in the electrochemical performance of ion batteries. Generally, cathode materials act as the lower-energy reservoir of electrons, determining the maximum discharge voltage, while anode materials have an important impact on the safety and long-term cycle life<sup>[22]</sup>. Until now, numerous materials, such as carbon materials<sup>[23, 24]</sup>, metal chalcogenide<sup>[25–27]</sup>, alloying materials<sup>[28, 29]</sup>, and organic materials<sup>[30, 31]</sup>, have been explored as electrode materials and have exhibited superior potential. Metal oxides are among the most widely studied electrode materials in PIBs because of their abundant types, adjustable compositions, and scalable preparation. Among them, vanadium oxides have attracted considerable interest. Vanadium has a variety of oxidation states varying from V<sup>2+</sup> to V<sup>5+</sup>, which provides multiple electron transfers during electrochemical reactions<sup>[32–34]</sup>. In the meantime, diverse oxidation states of vanadium, coordination geometries, and metal–oxygen connectivity make vanadium oxides show variegated framework structures and crystal chemistry. Most of the thermodynamically stable vanadium oxides are formed by infinite [VO<sub>6</sub>] octahedra sharing corners, faces, or edges. The [VO<sub>6</sub>] octahedra consisting of a long V–O bond (2.1–2.79 Å, 2.79 Å for V<sub>2</sub>O<sub>5</sub>) and a short V=O bond (1.55–1.75 Å) tend to be distorted into a square pyramid<sup>[35]</sup>. This distortion means that vanadium oxides feature various layered structures. These layered structures can provide natural rooms and pathways to accommodate and transfer metal ions<sup>[33]</sup>. Another key merit of vanadium oxides is low cost. Vanadium reserve is relatively abundant in Earth's crust, and meanwhile, the synthetic process of vanadium oxides is fa-



Scheme 1. (Color online) Schematic illustration of vanadium oxides for PIBs.

cile and efficient<sup>[32]</sup>. All of these factors make vanadium oxides become popular and promising candidates as electrode materials.

Until now, many vanadium oxides were investigated as electrode materials for PIBs and exhibited great potential. Nonetheless, the relevant research is insufficient in such an emerging battery field. More members of the vanadium oxide family are waiting to be explored. In addition, there is currently a lack of reviews to systematically summarize this kind of electrode material. Given these points, in this work, we highlight representative studies on vanadium oxides as PIB electrodes (including both cathode and anode) and introduce recent progress in brief (Scheme 1). Moreover, the electrochemical mechanism and performance improvement strategy of vanadium oxides are presented. Finally, based on current developments, the existing challenges and future opportunities are discussed. We hope that this review provides comprehensive information and understanding on vanadium oxides for PIBs and facilitates their future development.

## 2. Application in PIBs

### 2.1. V<sub>2</sub>O<sub>5</sub>

V<sub>2</sub>O<sub>5</sub> is the most studied vanadium oxide in metal-ion batteries. Likewise, it was attempted to be used as an electrode material in PIBs. Its electrochemical K storage possibility has been explored by a first principle study<sup>[36]</sup>. Four vanadium oxides were evaluated as PIB cathode materials, including  $\alpha$ -V<sub>2</sub>O<sub>5</sub>,  $\beta$ -V<sub>2</sub>O<sub>5</sub>, VO<sub>2</sub> (B), and VO<sub>2</sub> (R). Metastable  $\beta$ -V<sub>2</sub>O<sub>5</sub> showed a lower insertion energy and diffusion barrier for K<sup>+</sup> compared with the other three phases, which was attributed to its large interlayer distance, providing large interstitial sites to incorporate K<sup>+</sup>.  $\gamma$ -V<sub>2</sub>O<sub>5</sub> possesses the same orthorhombic symmetry as  $\alpha$ -V<sub>2</sub>O<sub>5</sub>, but benefiting from its larger interlayer spacing (~5 Å vs. 4.37 Å for  $\alpha$ -V<sub>2</sub>O<sub>5</sub>) and corrugated structure, it exhibits better electrochemical Li<sup>+</sup> and Na<sup>+</sup> storage performance<sup>[37–40]</sup>. In light of this, its electrochemical properties in PIBs were investigated. The insertion amount of K<sup>+</sup> in puckered layered  $\gamma$ -V<sub>2</sub>O<sub>5</sub> polymorph was up to 0.9 mol<sup>−1</sup> at a

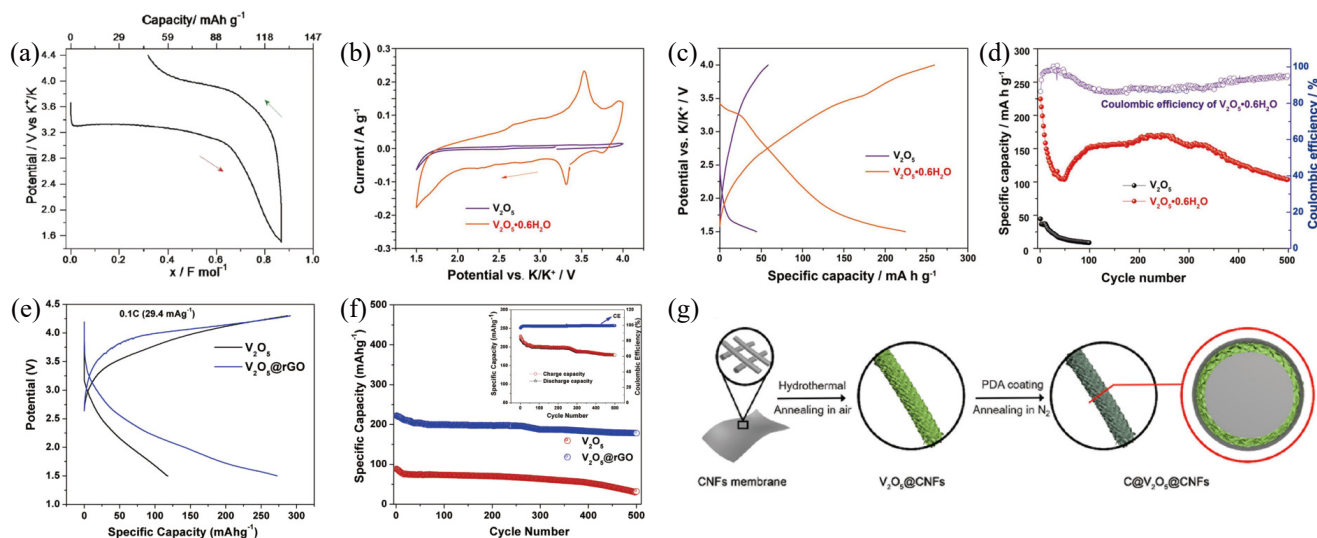


Fig. 1. (Color online) (a) First discharge/charge profile of  $\gamma$ - $V_2O_5$  in a 4.4–1.5 V voltage window<sup>[41]</sup>. Reprinted with permission, Copyright 2021, American Chemical Society. (b) First CV curves at a scan rate of 0.1 mV/s, (c) initial discharge/charge profiles, and (d) cycling performance of  $V_2O_5 \cdot 0.6H_2O$  and  $V_2O_5$  at 50 mA/g<sup>[42]</sup>. Reprinted with permission, Copyright 2018, American Chemical Society. (e) First charge/discharge profiles and (f) cycling performance of  $V_2O_5$  and  $V_2O_5@rGO$ <sup>[44]</sup>. Reprinted with permission, Copyright 2019, Elsevier. (g) Schematic illustration of the fabrication of  $C@V_2O_5@CNFs$ <sup>[46]</sup>. Reprinted with permission, Copyright 2022, Elsevier.

voltage range of 4.4–1.5 V at a high energy level of 3.3 V (Fig. 1(a)), which is very close to those of  $Li^+$  and  $Na^+$ <sup>[41]</sup>. During the first discharge, a series of layered  $K_xV_2O_5$  was formed, and  $K_{0.78}V_2O_5$  was finally obtained at 2.4 V. In the following cycling,  $K_xV_2O_5$  ( $0.3 \leq x \leq 0.78$ ) was responsible for K storage. The capacity maintained 48 mA·h/g after 100 cycles and only a slight structure change occurred. Structural water molecules in the interlayer are also a key factor in the electrochemical activity. They can expand the interlayer spacing effectively, which is in favor of the insertion and transfer of  $K^+$  with a large ionic radius. Taking  $V_2O_5 \cdot 0.6H_2O$  as an example, its interlayer spacing is 13.26 Å, being more than three times larger than that of  $V_2O_5$ <sup>[42]</sup>. Serving as a PIB cathode, there were significant differences in electrochemical performance, as shown in Figs. 1(b) and 1(c).  $V_2O_5$  showed very low capacity and inferior cycling stability (only 8.6 mA·h/g at the 100th cycle), while  $V_2O_5 \cdot 0.6H_2O$  delivered an initial capacity of 224.4 mA·h/g, and the capacity retention ratios kept 78.3% and 46.1% after 100 and 500 cycles, respectively (Fig. 1(d)).

In general,  $V_2O_5$  as an electrode material is limited by low electronic conductivity, which leads to sluggish reaction kinetics. Compositing with carbon materials is a feasible strategy to solve this issue. For instance, amorphous  $V_2O_5$  was uniformly coated on carbon nanotube (CNT) sponge via atomic layer deposition to form a core-shell structured  $V_2O_5@CNT$  composite. The  $V_2O_5@CNT$  cathode delivered a high initial capacity of 206 mA·h/g at 5 mA/g and a rate capacity of 60 mA·h/g at 200 mA/g<sup>[43]</sup>. Additionally, Nithya *et al.* utilized reduced graphene oxide (rGO) to modify  $V_2O_5$  nanorod ( $V_2O_5@rGO$ )<sup>[44]</sup>. As the cathode of PIBs, the specific capacity and cycling stability of  $V_2O_5@rGO$  were enhanced obviously compared with those of pure  $V_2O_5$  (Figs. 1(e) and 1(f)). After 500 cycles, the capacity retention retained 80%. Morphology regulation that can effectively improve the electrochemical performance of electrode materials is also adopted by  $V_2O_5$ . Micron-sized nanoporous  $V_2O_5$  arrays are synthesized using  $V_2CT_x$  MXene as a precursor by one-step annealing treat-

ment. It had similar specific capacities in the first few cycles as commercial  $V_2O_5$ . However, in the following cycling processes, the capacity of commercial  $V_2O_5$  gradually dropped and the capacity retention was only 13% after 90 cycles, which was far below that of the micron-sized nanoporous  $V_2O_5$  arrays (86.72%)<sup>[45]</sup>.

$V_2O_5$  was also used as PIB anodes. Zhou *et al.* designed a freestanding anode material of carbon-coated  $V_2O_5$  nanosheets vertically loaded on carbon fibers ( $C@V_2O_5@CNFs$ ) (Fig. 1(g))<sup>[46]</sup>. In rate tests, the capability of pure  $V_2O_5$  nanosheets at each energy density was much lower than that of  $V_2O_5@CNFs$  and  $C@V_2O_5@CNFs$ . Compared with  $C@V_2O_5@CNFs$ ,  $V_2O_5@CNFs$  had higher capacities at low current densities but lower capacities at high current densities. In the following cycling test, the capacity of  $C@V_2O_5@CNFs$  was still 276 mA·h/g after ~800 cycles, while  $V_2O_5@CNFs$  could only deliver 34 mA·h/g after 400 cycles. The obviously different cycling stability between these two materials was attributed to the protection of the carbon coating toward the structure of the  $V_2O_5$  nanosheets. Impressively, long-term cycle testing featured a capacity of ~139 mA·h/g at 2000 mA/g after 5000 cycles.

## 2.2. $VO_2$

$VO_2$  is arranged in an up-down-up-down chess-board-like manner and shows a similar layered structure to  $V_2O_5$ . It has more than ten phases, among which brookite phase  $VO_2$ , denoted as  $VO_2$  (B), is the most studied one<sup>[47, 48]</sup>. The layered  $VO_2$  (B) is composed of  $[VO_6]$  octahedron bilayers that are connected by sharing corners. The  $VO_2$  (B) structure has plentiful one-dimensional (1D) channels between the layers, providing superior ion diffusion pathways, and thus  $VO_2$  (B) has been widely used in metal-ion batteries<sup>[49, 50]</sup>. Recently, Lu and co-workers investigated its electrochemical K storage properties as an anode for the first time<sup>[51]</sup>. Based on the results of density functional theory (DFT) calculations, they constructed surface-amorphized  $VO_2$  nanorods (SA- $VO_2$ ) consisting of a crystalline core and an amorphous shell by an interfa-

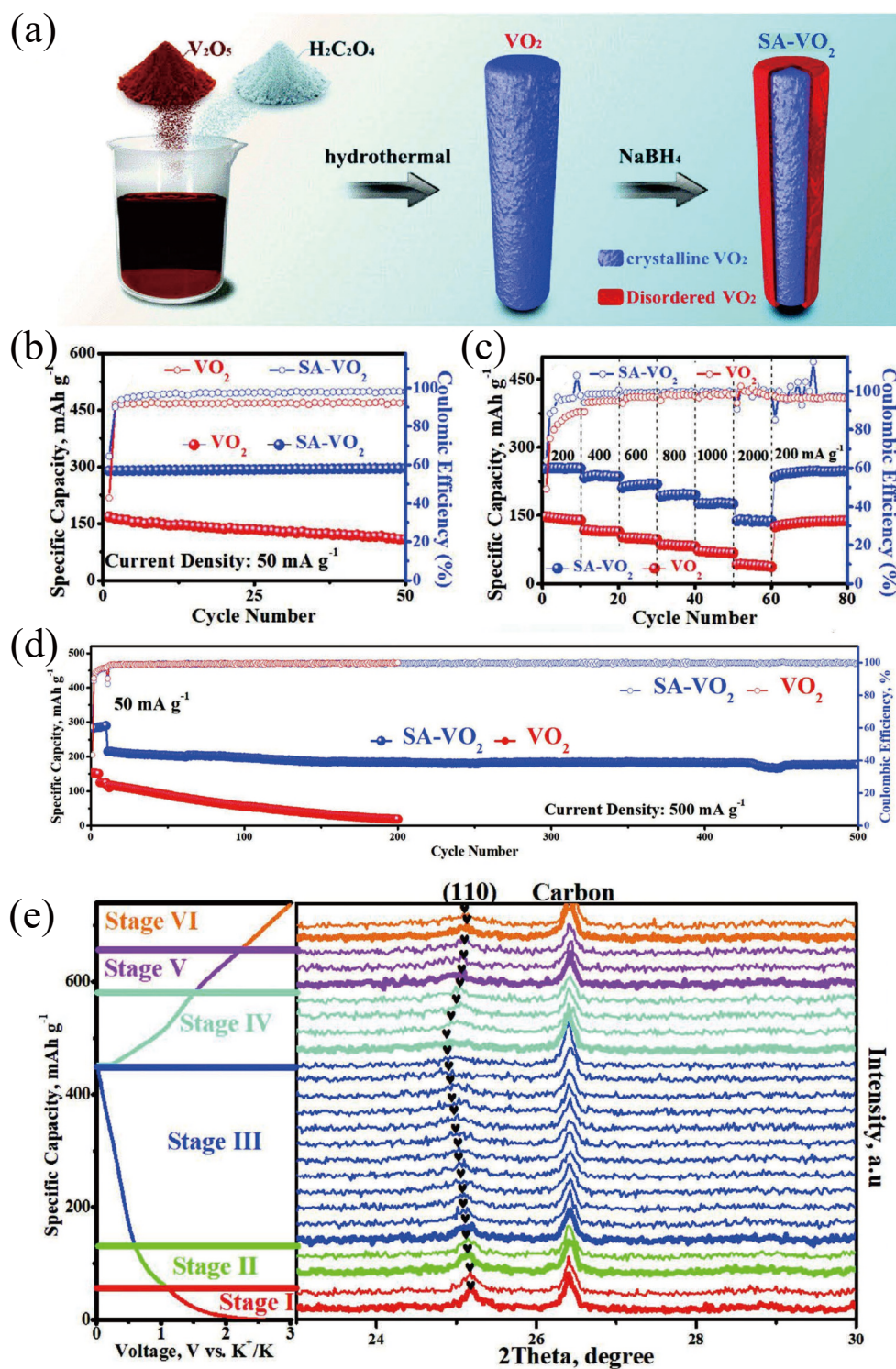


Fig. 2. (Color online) (a) Schematic of the synthesis of SA-VO<sub>2</sub>. (b) Cycling performance, (c) rate performance, and (d) long-term cycling stability of SA-VO<sub>2</sub> and VO<sub>2</sub>. (e) In situ XRD patterns of SA-VO<sub>2</sub> anode operated at different charge states<sup>[51]</sup>. Reprinted with permission, Copyright 2020, Wiley.

cial engineering strategy (Fig. 2(a)). The interaction between the crystalline core and the oxygen-rich defect amorphous shell generated large intimate heterointerface, which could decrease the surface energy, narrow the band gap, and reduce the K<sup>+</sup> diffusion barrier. Moreover, the heterointerface provided extra active sites for K<sup>+</sup>. All of these enable SA-VO<sub>2</sub> to exhibit a higher specific capacity, rate capability, and long-term stability compared with pure VO<sub>2</sub> (Figs. 2(b)–2(d)). Moreover, the structural stability of SA-VO<sub>2</sub> was much better

than that of VO<sub>2</sub>. After cycling 100 times, pure VO<sub>2</sub> was severely pulverized, fractured, and agglomerated, and its crystal structure was destroyed. However, SA-VO<sub>2</sub> could keep its morphology and crystal structure. In addition, in situ X-ray diffractometer (XRD) analysis indicated that the electrochemical K<sup>+</sup> storage of SA-VO<sub>2</sub> was governed by an intercalation reaction (Fig. 2(e)). Subsequently, triclinic VO<sub>2</sub> was explored as the anode of PIBs by Meng *et al.*<sup>[52]</sup>. In their work, a freestanding VO<sub>2</sub>/carbon foam (VOCF) composite was prepared via a hy-

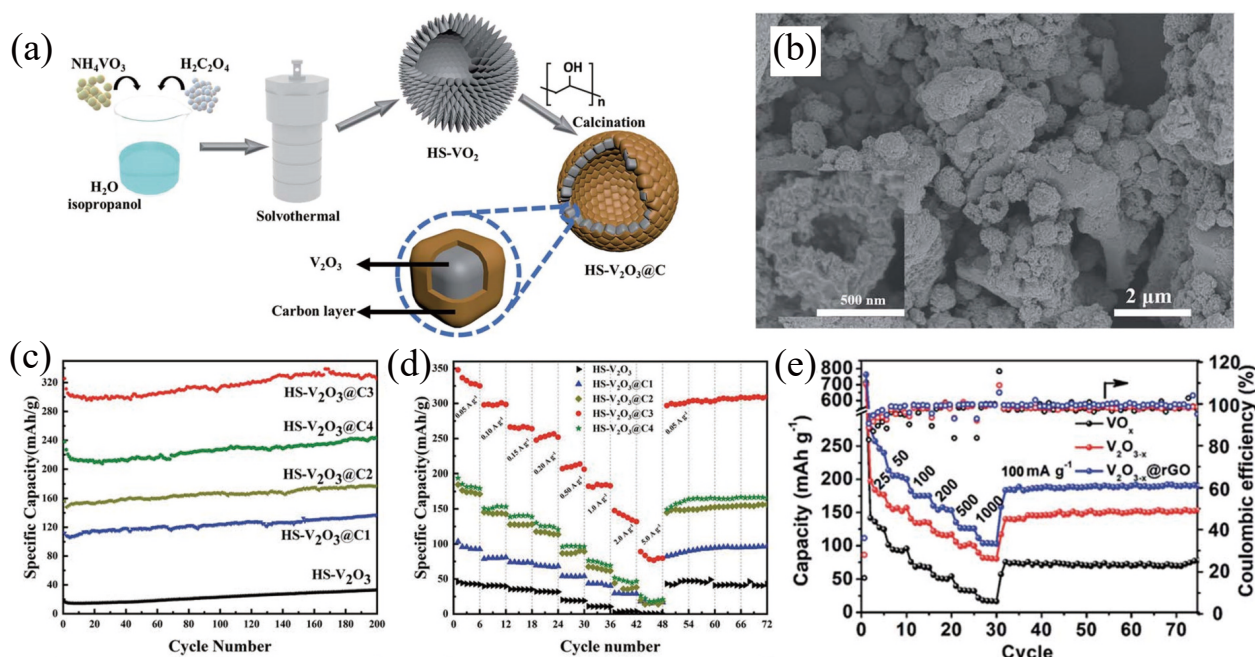


Fig. 3. (Color online) (a) Schematic preparation route of HS-V<sub>2</sub>O<sub>3</sub>@C. (b) Scanning electron microscopy (SEM) image of HS-V<sub>2</sub>O<sub>3</sub>@C. (c) Cycling and (d) rate performance of samples with different carbon contents<sup>[53]</sup>. Reprinted with permission, Copyright 2020, The Royal Society of Chemistry. (e) Rate performance of VO<sub>x</sub>, V<sub>2</sub>O<sub>3-x</sub>, and V<sub>2</sub>O<sub>3-x</sub>@rGO<sup>[55]</sup>. Reprinted with permission, Copyright 2019, The Royal Society of Chemistry.

drothermal method, in which the 3D conductive network provided electron transport pathways and the porous structure promoted electrolyte penetration. Its electrochemical mechanism was also the intercalation/de-intercalation process of K<sup>+</sup>. Impressively, its capacities could maintain 372.0 and 247.6 mA·h/g at 0.1 and 0.2 A/g after 200 cycles, respectively. Long-term testing at 1.0 A/g featured 65.7% retention after 400 cycles.

### 2.3. V<sub>2</sub>O<sub>3</sub>

V<sub>2</sub>O<sub>3</sub> has a rhombohedral corundum structure at an ambient temperature where V atoms form 3D V-V, and O atoms form distorted octahedrons around the V atoms. In the reported work, V<sub>2</sub>O<sub>3</sub> was used as PIB anodes. It is largely restricted by the low electronic conductivity and the relatively large volume changing. To address these problems, highly conductive carbon materials are usually incorporated to form composites. For example, Chen's group designed carbon-coated V<sub>2</sub>O<sub>3</sub> hollow spheres (HS-V<sub>2</sub>O<sub>3</sub>@C) (Figs. 3(a) and 3(b))<sup>[53]</sup>. The role of carbon contents was studied first. In comparison with HS-V<sub>2</sub>O<sub>3</sub>, HS-V<sub>2</sub>O<sub>3</sub>@C samples with different carbon contents exhibited better electrochemical performance. The capacity increased with the increase of the carbon content, but the capacity decreased when the carbon content was excessive. The enhanced electrochemical performance was attributed to the improved electronic conductivity derived from the carbon coating layer. Nonetheless, the capacity of the carbon coating layer was lower than that of V<sub>2</sub>O<sub>3</sub>, which had a negative impact on the capacity of the composites (Figs. 3(c) and 3(d)). Subsequently, bulk V<sub>2</sub>O<sub>3</sub> with almost the same carbon coating content (B-V<sub>2</sub>O<sub>3</sub>) was prepared and used to investigate the effect of the morphology of V<sub>2</sub>O<sub>3</sub>. As a result, the optimal HS-V<sub>2</sub>O<sub>3</sub>@C showed better electrochemical performance in specific capacities, cycling stability, and rate capability. Two reasons could explain this: 1) the smaller size of HS-V<sub>2</sub>O<sub>3</sub>@C was in favor of electron and ion diffusion; 2) the primary particles

of HS-V<sub>2</sub>O<sub>3</sub>@C were smaller and not compact to each other, and thus the carbon layers could coat each primary particle. In addition, various engineering strategies are combined with carbon modification to further enhance the structural stability and accelerate K<sup>+</sup> reaction kinetics, such as heteroatom doping<sup>[54]</sup>, creating defects<sup>[55]</sup>, and morphology design<sup>[54]</sup>. For example, highly defective V<sup>2+</sup>-doping V<sub>2</sub>O<sub>3-x</sub> nanofiber bundles could deliver better rate capability at a wide current density range between 25 to 1000 mA/g than pure V<sub>2</sub>O<sub>3</sub> (Fig. 3(e))<sup>[55]</sup>. The rate capacities could be improved when rGO was introduced.

### 2.4. K<sub>x</sub>V<sub>2</sub>O<sub>5</sub>

K<sub>x</sub>V<sub>2</sub>O<sub>5</sub> is a group of vanadium oxides, where *x* is a variable value and below 1. It is reported that the preintercalation of K<sup>+</sup> in V<sub>2</sub>O<sub>5</sub> could enlarge and stabilize the diffusion channel, thus resulting in enhanced electrochemical cycling and rate performance in LIBs<sup>[56]</sup>. Along this line, K<sup>+</sup>-preintercalated V<sub>2</sub>O<sub>5</sub> was expected to show superior electrochemical K storage in PIBs. Bilayered δ-V<sub>2</sub>O<sub>5</sub>·*n*H<sub>2</sub>O with an interlayer spacing of 9.62 Å was first tried to be chemically preintercalated with K<sup>+</sup><sup>[57]</sup>. After K<sup>+</sup> intercalation, single-phase bilayered δ-K<sub>0.42</sub>V<sub>2</sub>O<sub>5</sub>·*n*H<sub>2</sub>O was obtained and the interlayer spacing was expanded to 9.65 Å. The large interlayer spacing and well-defined intercalation sites formed by K<sup>+</sup> intercalation contributed to a high capacity, which was better than previous cathode materials. Afterward, 1D bilayered δ-K<sub>0.51</sub>V<sub>2</sub>O<sub>5</sub> nanobelts with an interlayer spacing of 9.5 Å and optimized growth orientation along the [010] direction were prepared by reconstructing the V-O polyhedra of α-V<sub>2</sub>O<sub>5</sub> (Figs. 4(a)–4(c))<sup>[58]</sup>. The structural properties theoretically were beneficial for K<sup>+</sup> insertion/extraction and diffusion. Serving as a PIB cathode, their average voltage reached 3.2 V and exhibited a high capacity (131 mA·h/g) and rate capability (64 mA·h/g at 10 A/g). DFT calculations confirmed that such superior electrochemical performance was attributed to low diffusion barriers and short

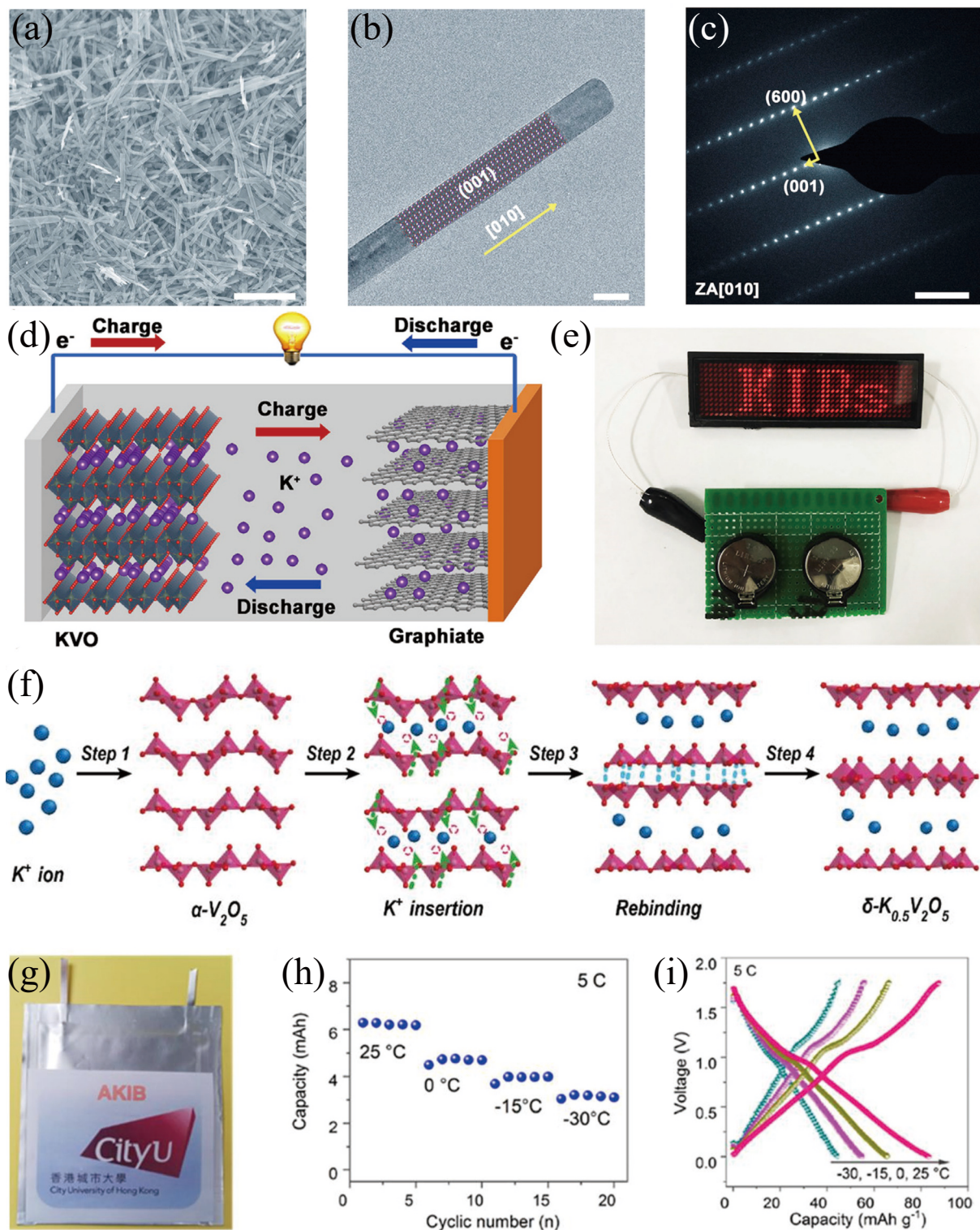


Fig. 4. (Color online) (a–c) SEM, transmission electron microscopy, and selected area electron diffraction images of  $\delta\text{-K}_{0.51}\text{V}_2\text{O}_5$ . (d) Schematic illustration of  $\delta\text{-K}_{0.51}\text{V}_2\text{O}_5$ /graphite full cell and (e) Light-emitting diode (LED) screen is driven by the full cell<sup>[58]</sup>. Reprinted with permission, Copyright 2019, Elsevier. (f) Structural evolution of the reconstructing process from  $\alpha\text{-V}_2\text{O}_5$  to  $\delta\text{-K}_{0.5}\text{V}_2\text{O}_5$ . (g) Digital image of  $\delta\text{-K}_{0.5}\text{V}_2\text{O}_5$ /PTCDI pouch cell. (h) Cycling performance and (i) corresponding discharge/charge curves of the pouch cell at different temperatures<sup>[59]</sup>. Reprinted with permission, Copyright 2021, American Chemical Society.

diffusion length caused by the large interlayer spacing and unique 1D structure along the [010] orientation. The as-prepared  $\delta\text{-K}_{0.51}\text{V}_2\text{O}_5$  cathode was further used to assemble a PIB full cell using a graphite anode (Figs. 4(d) and 4(e)). The full cell delivered a high energy density (238 W-h/kg) and power density (5480 W/kg). Reconstructed  $\delta\text{-K}_{0.5}\text{V}_2\text{O}_5$  nanobelts also displayed great electrochemical K storage capability in

aqueous systems (Fig. 4(f))<sup>[59]</sup>. In a 22 M  $\text{KCF}_3\text{SO}_3$  water-in-salt electrolyte, the rate capacities of the  $\delta\text{-K}_{0.5}\text{V}_2\text{O}_5$  electrode at 1 and 50 C were 116 and 65 mA-h/g, respectively, corresponding to a 56% capacity retention. The capacity still maintained 102 mA-h/g with 88.2% capacity retention after 1000 cycles. In addition, an assembled  $\delta\text{-K}_{0.5}\text{V}_2\text{O}_5$ /perylene-tetracarboxylic diimide (PTCDI) aqueous PIB full cell had excellent electro-

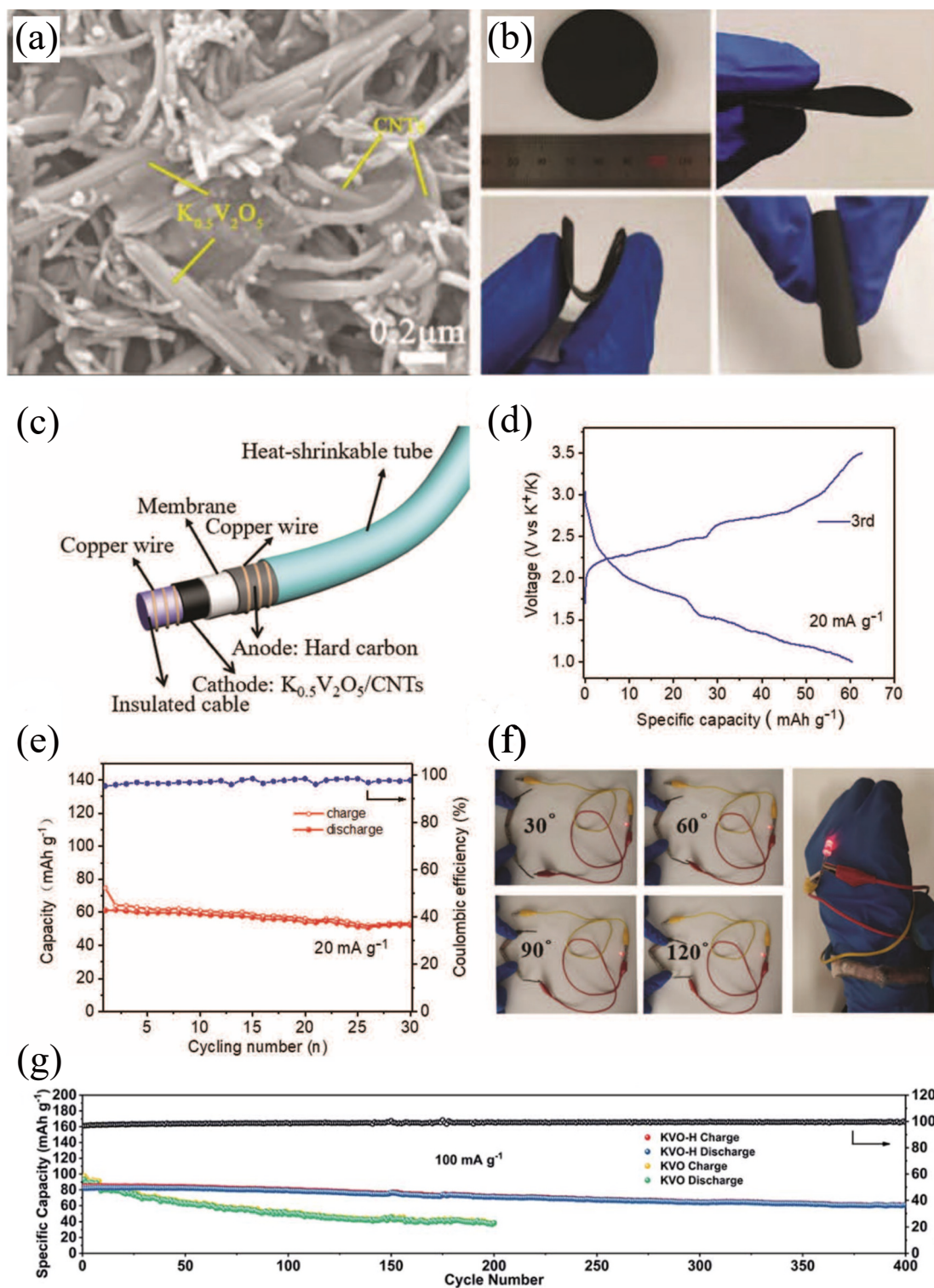


Fig. 5. (Color online) (a) SEM images of  $K_{0.5}V_2O_5/CNTs$  hybrid film. (b) Optical images of  $K_{0.5}V_2O_5/CNT$  film at different bending states. Flexible cable-shaped  $K_{0.5}V_2O_5/CNTs$ /hard carbon PIB full cell: (c) schematic diagram of the structure, (d) the charge/discharge curve at the 3rd cycle, (e) the cycling stability and coulombic efficiency, and (f) photographs of a red LED powered by the cable-shaped PIB at various bending angles<sup>[61]</sup>. Reprinted with permission, Copyright 2021, The Royal Society of Chemistry. (g) Cycling performance of  $\delta$ - $K_{0.5}V_2O_5$  and  $K_{0.5}V_2O_5 \cdot 0.5H_2O$ <sup>[63]</sup>. Reprinted with permission, Copyright 2021, The Royal Society of Chemistry.

chemical performance. Impressively, the full cell could work at different temperatures (Figs. 4(g)–4(i)). Generally, cathode materials with high K content are beneficial to the energy density of full cells, since all  $K^+$  involved in electrochemical reaction will be supplied by the cathode material in practice. Therefore, a high K-containing vanadium oxide  $K_{0.83}V_2O_5$  was developed and applied as the cathode of PIBs<sup>[60]</sup>. Although

its electrochemical performance was not better than the previously reported  $K_xV_2O_5$  that was obtained at temperatures over 200 °C, it could be synthesized by a facile chemical potasiation under ambient conditions.

Nonetheless,  $K_xV_2O_5$  is restricted by serious volume expansion and inferior electronic conductivity, which result in unsatisfactory structural stability and fast capacity decay during re-

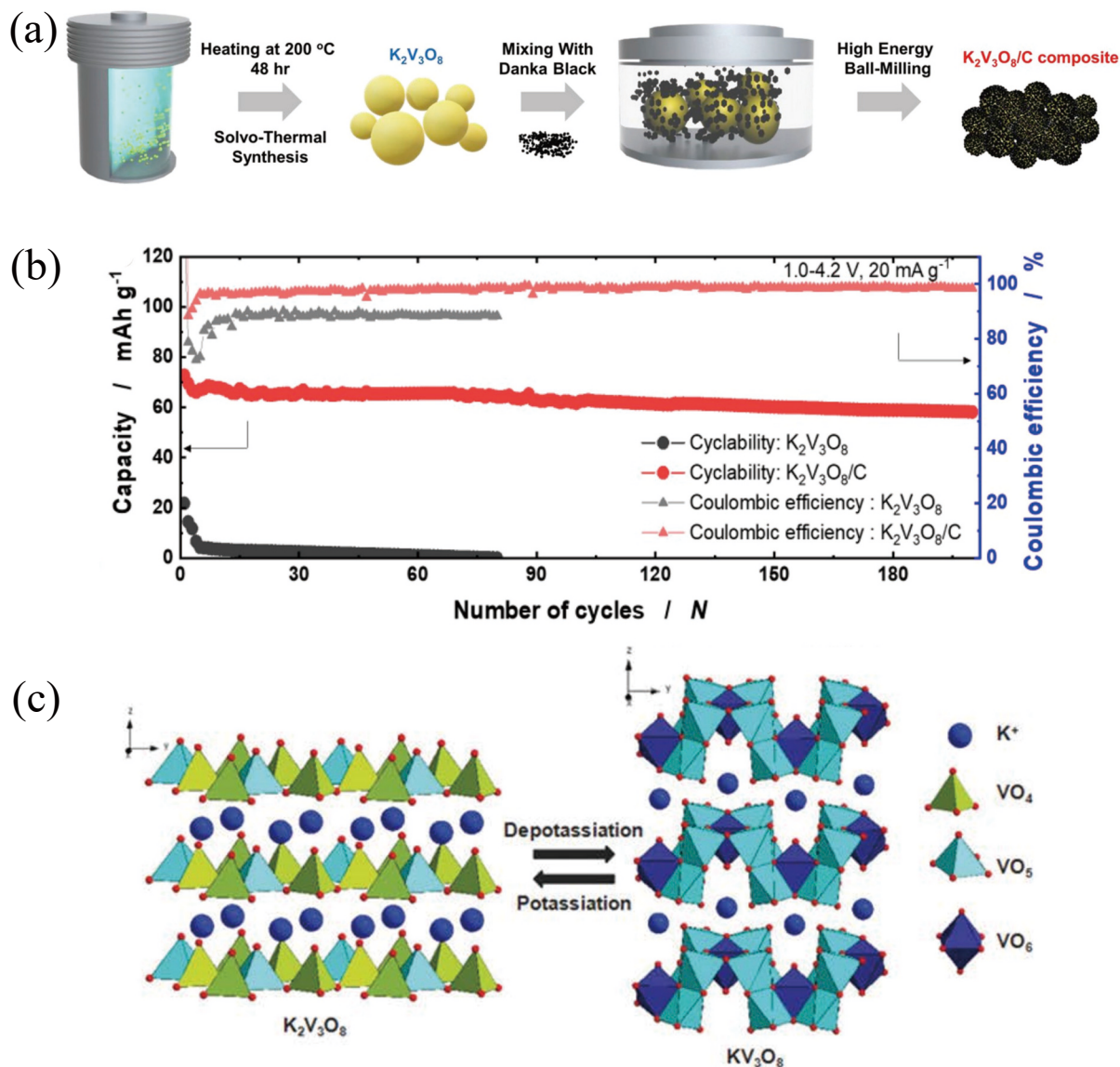


Fig. 6. (Color online) (a) Schematic of the synthesis of  $K_2V_3O_8/C$  composite. (b) Cycling stability of  $K_2V_3O_8/C$  and  $K_2V_3O_8$ <sup>[66]</sup>. Reprinted with permission, Copyright 2019, Elsevier. (c) Schematic illustration of the phase transition between  $K_2V_3O_8$  and  $KV_3O_8$ <sup>[67]</sup>. Reprinted with permission, Copyright 2019, The Royal Society of Chemistry.

peated cycling. Incorporating conductive materials is a feasible option to offset these problems. Xu and co-workers designed a  $K_{0.5}V_2O_5$  nanobelts/CNT flexible film (Figs. 5(a) and 5(b)) and applied it as a PIB cathode<sup>[61]</sup>. The flexible and interconnected network structure not only provided good ion and electron transport paths but also played as an elastic medium to buffer the volume change of  $K_{0.5}V_2O_5$ . The hybrid film was able to deliver a cycling capacity of 80 mA·h/g at 50 mA/g after 100 cycles and an exceptional rate capacity of 63 mA·h/g at 500 mA/g. A long-term cycling test at 500 mA·h/g featured 51 mA·h/g after 300 cycles. Moreover, it exhibited good electrochemical performance in a full cell where a potassiated hard carbon was used as the anode. To expand its practical application, a flexible cable-shaped PIB full cell was constructed. The full cell could retain 51 mA·h/g after 30 cycles and light a commercial red LED at different bending angles, as shown in Figs. 5(c)–5(f). Deng *et al.* synthesized a conductive polyacrylonitrile (PAN) coating  $K_{0.486}V_2O_5$  composite and annealed it at different temperatures<sup>[62]</sup>. The

PAN coating layer with a feasible annealing temperature possessed the elastic properties of the PAN precursor, which could relieve the volume expansion of  $K_{0.486}V_2O_5$ . In the meanwhile, the coating layer could accelerate electron transport and inhibit the decomposition of organic electrolytes. Additionally, it is reported that the capacity decay of potassium vanadium oxides arises from the amorphization of their crystal structure during repeated depotassiation–potassiation processes<sup>[63]</sup>. To this end, nanocrystalline  $K_{0.5}V_2O_5 \cdot 0.5H_2O$  with interlayered water was prepared by turning synthesis conditions. Employing as PIB cathodes, the capacity retention of  $K_{0.5}V_2O_5 \cdot 0.5H_2O$  nanocrystalline reached 74% after 400 cycles, whereas the capacity retention of  $\delta$ - $K_{0.5}V_2O_5$  was only 41.3% after 200 cycles (Fig. 5(g)). In rate performance testing,  $K_{0.5}V_2O_5 \cdot 0.5H_2O$  nanocrystalline delivered higher capacities than  $\delta$ - $K_{0.5}V_2O_5$  at all current densities. The authors pointed out that by reducing the long-range structural order in highly crystalline  $\delta$ - $K_{0.5}V_2O_5$ , the electrochemical storage mechanism changed from battery-type intercalation accompanied by



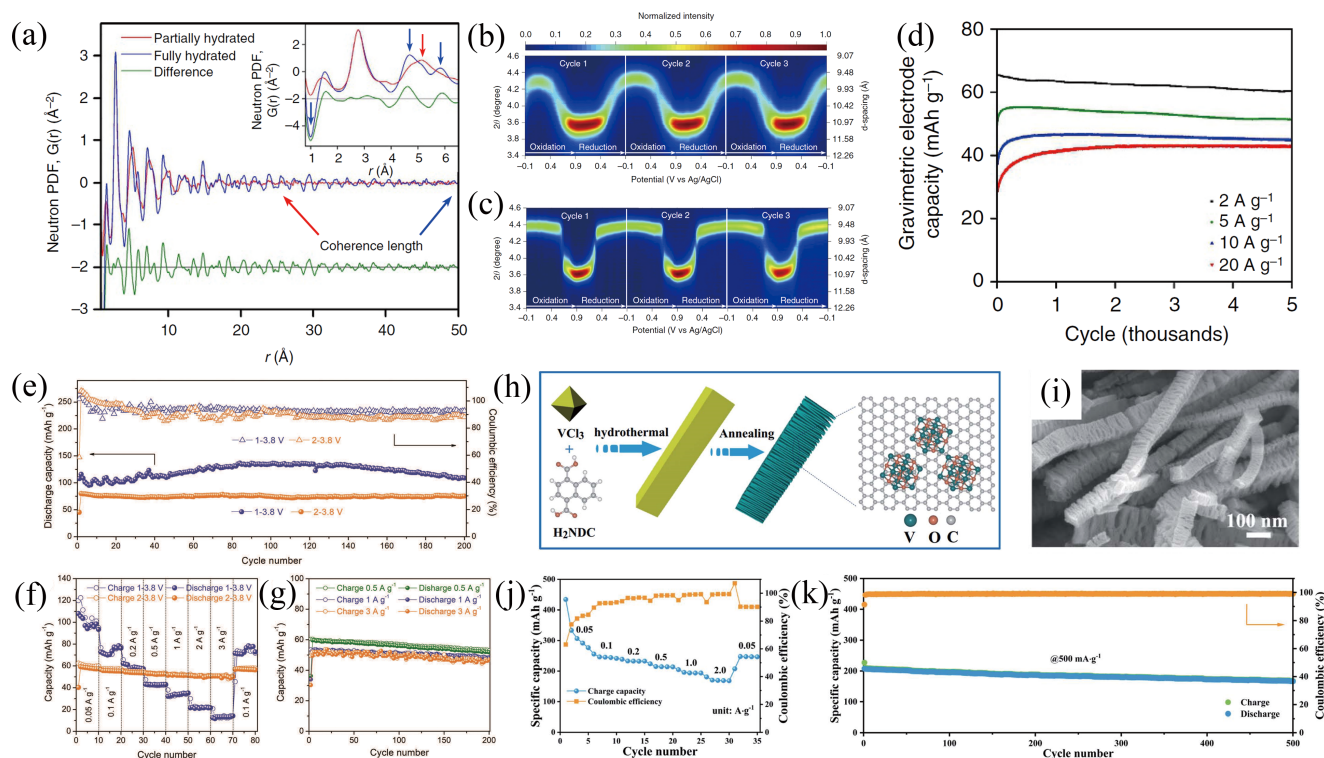


Fig. 7. (Color online) (a) Neutron PDFs of partially and fully hydrated disordered  $K_{0.22}V_{1.74}O_{4.37} \cdot 0.82H_2O$ . (b, c) In situ XRD spectra of the layered (001) plane during cycling. (d) The average gravimetric electrode capacity through the 5000 cycles at different current densities<sup>[68]</sup>. Reprinted with permission, Copyright 2017, Springer Nature. (e, f) Cycling performance and rate capability of  $NH_4V_4O_{10}$  in 1/2–3.8 V. (g) Cycling performance of  $NH_4V_4O_{10}$  at high rates in 2–3.8 V<sup>[69]</sup>. Reprinted with permission, Copyright 2019, Wiley. (h, i) Schematic illustration of the synthetic process and SEM image of VO/C. (j, k) Rate and cycling performance of KPBB/VO/C full cell<sup>[71]</sup>. Reprinted with permission, Copyright 2020, The Royal Society of Chemistry.

the phase transition in  $\delta-K_{0.5}V_2O_5$  to phase transition-free pseudocapacitive  $K^+$  intercalation in  $K_{0.5}V_2O_5 \cdot 0.5H_2O$ . DFT calculations indicated that the water in the interlayer spacing effectively suppressed the phase transition of  $K_{0.5}V_2O_5 \cdot 0.5H_2O$  during electrochemical reactions and thus largely diminished the mechanical damage. According to these points, the electrochemical performance was enhanced.

$K_xV_2O_5$  also shows great potential as a PIB anode material.  $K_{0.23}V_2O_5$  was prepared and investigated as LIB and PIB anodes by Luo's group<sup>[64]</sup>. In these two battery systems, it presented good ion storage behaviors. However, the charge storage mechanisms were quite different. In PIBs, there was only an intercalation reaction. K storage capacities of 121.6 and 97.4 mA·h/g could be preserved at 20 and 100 mA/g after 150 and 100 cycles, respectively.

## 2.5. $K_2V_3O_8$

$K_2V_3O_8$  is another kind of potassium vanadium oxide and was first introduced as an anode material for PIBs<sup>[65]</sup>. It delivered a high initial capacity of  $\sim 300$  mA·h/g. However, its cycling stability was not satisfactory; the capacity gradually decreased to  $\sim 84$  mA·h/g within the following 180 cycles, corresponding to only 31.1% capacity retention. As for rate capability, the reversible capacities of 300, 242, 192, 124, and 103 mA·h/g were obtained at the current densities of 50, 100, 200, 400, and 500 mA/g, respectively. Thereafter, given the unique structure of  $K_2V_3O_8$ , arranged with alternating K–O layers and V–O layers along the  $c$ -axis,  $K_2V_3O_8$  was explored as a

PIB cathode<sup>[66]</sup>. To improve the electrical conductivity,  $K_2V_3O_8$  was modified by carbon black via a high-energy ball milling method (Fig. 6(a)), namely  $K_2V_3O_8/C$ . In theory, the specific capacity of  $K_2V_3O_8$  is 149.2 mA·h/g. However, the as-prepared  $K_2V_3O_8$  only delivered a capacity of 22 mA·h/g. In contrast, the capacity of  $K_2V_3O_8/C$  was 75 mA·h/g. In addition, its capacity retention was retained at  $\sim 80\%$  after 200 cycles (Fig. 6(b)). The  $K_2V_3O_8/C$  cathode was further paired with a hard carbon anode to fabricate a full cell. In a voltage range of 0.5–3.8 V, the full cell exhibited an initial capacity of 61 mA·h/g and 87% capacity retention after 50 cycles. Another work reported that  $K_2V_3O_8$  without any modification could deliver a reversible capacity of 100 mA·h/g in a voltage range of 1.5–4.5 V with an average discharge voltage of 2.7 V and retained 73% capacity retention after 50 cycles<sup>[67]</sup>. Mechanism studies indicated that  $K_2V_3O_8$  experienced a non-topotactic process accompanied by a reversible phase transition between  $KV_3O_8$  and  $K_2V_3O_8$  during depotassiation and potassiation (Fig. 6(c)). Meanwhile, a 23.4% volume change occurred, thus leading to the mechanical failure and slow capacity decay.

## 2.6. Other vanadium oxides

Other vanadium oxides such as  $NH_4V_4O_{10}$ ,  $H_2V_3O_8$ , and binary vanadium oxide heterostructures have also been investigated as electrode materials for PIBs. However, they have not received much attention, and thus the related reports are limited. Potassium-intercalated disordered vanadium oxide nanosheets engaged by structural water ( $K_{0.22}V_{1.74}O_{4.37} \cdot 0.82H_2O$ ) are the earliest studied vanadium ox-

ides for aqueous electrochemical K storage<sup>[68]</sup>. Ex situ and in situ neutron and X-ray scattering measurements demonstrated that the interaction between the disordered structure and the structural water within the interlayer enhanced the stability and electrochemical performance (Figs. 7(a)–7(c)). It achieved a K storage capacity of 183 mA·h/g in half cells and preserved nearly 100% capacity retention over 5000 cycles at various current densities in full cells (Fig. 7(d)).  $\text{NH}_4\text{V}_4\text{O}_{10}$ , a layered vanadium oxide, was synthesized and investigated as a PIB cathode by Lei's group<sup>[69]</sup>. It featured a large interlayer spacing of 9.8 Å and a flower-like architecture, which was in favor of  $\text{K}^+$  diffusion and provided structural stability to endure long-term electrochemical cycling. Electrochemical mechanism studies in different voltage ranges revealed that the instability of the layered structure arose from the deammoniation from the interlayer space and the capture of  $\text{K}^+$  in the interlayer space. According to this result, the improved electrochemical performance was realized by a controlling voltage window (Figs. 7(e) and 7(f)). It exhibited superior cycling stability at 0.5, 1, and 3 A/g for 200 cycles in the optimized voltage window (Fig. 7(g)).  $\text{H}_2\text{V}_3\text{O}_8$  was applied as a cathode material for PIBs and could deliver capacities of 168 and 109 mA·h/g at the 1st and 100th cycles at 10 mA/g, respectively<sup>[70]</sup>. Its crystal structure had good reversibility during cycling. Chen and co-workers employed a metal-organic framework as a precursor to construct a spring-like lamellar VO nanoparticle/amorphous carbon composite (VO/C) (Figs. 7(h) and 7(i)).<sup>[71]</sup> The unique nanostructure endowed the material with strong structural rigidity to alleviate large volume variation during electrochemical reactions. In the meanwhile, the hybrid structure effectively increased the conductivity and decreased the  $\text{K}^+$  diffusion barrier. In this case, VO/C produced capacities of 345 mA·h/g at 0.1 A/g after 400 cycles and 241 mA·h/g at 1 A/g after 1000 cycles when it served as the anode of PIBs. Concerning the rate performance, its capacity reached 104 mA·h/g at a high current density of 15 A/g. More importantly, a full cell assembled by the VO/C anode and a Prussian blue analogue (KPB) cathode displayed great application prospects. As shown in Figs. 7(j) and 7(k), the full cell had excellent rate performance and cycling stability. Another research on PIB anodes reported an amorphous  $\text{VO}_x$  encapsulated into defective carbon nanofibers<sup>[72]</sup>. The structural amorphization of  $\text{VO}_x$  and the defect of carbon matrices synergistically provided abundant active sites and multi-channels for ion storage and diffusion and alleviated electrode pulverization caused by structural changing. Electrochemical tests revealed that the sample with the optimized annealing temperature possessed great cycling stability (198 mA·h/g at 0.5 A/g after 400 cycles) and rate performance (170 mA·h/g at 1 A/g).

Binary vanadium oxide heterostructures have also been explored for use as the electrode of PIBs because their interface effect and the built-in electric field at the heterointerface could alleviate interfacial stress and promote reaction kinetics. For example, Cao *et al.* prepared 3D N-doped carbon networks encapsulated  $\text{VO}_2\text{-V}_2\text{O}_5$  heterostructures ( $\text{VO}_2\text{-V}_2\text{O}_5/\text{NC}$ )<sup>[73]</sup>. Employing as a PIB anode,  $\text{VO}_2\text{-V}_2\text{O}_5/\text{NC}$  presented better electrochemical performance including specific capacities and rate capability compared with  $\text{V}_2\text{O}_5/\text{NC}$ ,  $\text{VO}_2/\text{NC}$ , and NC. The  $\text{VO}_2\text{-V}_2\text{O}_5/\text{NC}$  electrode could maintain 256 mA·h/g with

100% Coulombic efficiency after 1600 repeated charge–discharge cycles. Recently, carbon-coated  $\text{VO}_2/\text{V}_2\text{O}_5$  nanoparticles ( $\text{VO}_2/\text{V}_2\text{O}_5@\text{C}$ ) were fabricated and used as the anode material of PIBs<sup>[74]</sup>. As a result, they delivered good electrochemical K storage capability in both half and full cells.

### 3. Promising improvement strategies

Although vanadium oxides as PIB electrode materials achieved encouraging results as presented in Section 2, there seems to be large room for the electrochemical performance and structural stability improvement. Therefore, this section will summarize the effective strategies used in PIBs and introduce some promising strategies realized by other battery systems, which may provide a feasible route to promote the development of vanadium oxides in PIBs.

#### 3.1. Carbon material coating

Vanadium oxides as an electrode material are confronted with severe volume expansion, which may lead to electrode pulverization, voltage hysteresis, and capacity fading. This problem is exacerbated in PIBs due to the larger ionic radius of  $\text{K}^+$ . In addition, they are restricted by sluggish reaction kinetics caused by their low electronic conductivity. Carbon material coating is a desirable choice to solve these issues. For one thing, the confinement effect of carbon material coating can effectively buffer the volume change of vanadium oxides<sup>[53, 72]</sup>. For another thing, generally, carbon materials have excellent conductivity, which can facilitate charge transfer<sup>[43, 44]</sup>. Furthermore, some carbon materials with characteristic properties, such as heteroatom-doped<sup>[73]</sup>, porous<sup>[75]</sup>, and defective<sup>[72]</sup>, can provide additional advantages for electrochemical reactions.

#### 3.2. Morphology design

Morphologies play a critical role in electrode materials and, certainly, this also applies to vanadium oxides. Well-designed morphologies could endow them with novel material properties. For instance, nanosized vanadium oxides expose large surface areas, which provide abundant active sites for electrochemical reactions. In addition, their ion and electron transmission capability can be improved because of the shortened diffusion length. Moreover, some special morphologies, such as hollow, porous, and hierarchical, have enough room to accommodate volume expansion. These features guarantee fast reaction kinetics and structural stability<sup>[3, 76, 77]</sup>.

#### 3.3. Defect engineering and heteroatom doping

Defect engineering and heteroatom doping have been widely used in various metal oxides. Defect engineering can create abundant metal or oxygen vacancies, which reduce the strong electrostatic interaction between host materials and ions, thereby accelerating reaction kinetics and promoting the reversible storage of ions<sup>[55, 78]</sup>. In addition, defects have a positive effect on improving the electronic conductivity of vanadium oxides<sup>[79]</sup>. As for heteroatom doping, it was demonstrated that the electronic conductivity and cycle stability of heteroatom-doped materials were much higher than those of undoped materials<sup>[80]</sup>. Moreover, heteroatom doping can expand the interlayer spacing of layered vanadium oxides, which is conducive to ion diffusion<sup>[81]</sup>. At present, various elements (e.g. copper<sup>[80]</sup>, iron<sup>[81]</sup>, and manganese<sup>[82]</sup>)

have been utilized as dopants and exhibited obvious enhancement for material structures and electrochemical behaviors.

### 3.4. Interlayer expansion

The majority of vanadium oxides possess a layered structure. Their interlayer space allows the intercalation of guest species and provides natural assets and pathways for ion storage and diffusion. It is well-known that larger interlayer spacing facilitates ion transfer. Therefore, the strategy of expanding the interlayer is feasible to enhance the electrochemical performance of vanadium oxides. This can be accomplished by preintercalating metal ions<sup>[57]</sup>, introducing structural water<sup>[42]</sup>, and doping heteroatoms<sup>[81]</sup>. Additionally, inserting organic molecules/polymers into the interlayer spacing is a superior option. Another key feature is that the designability of organic molecules/polymers makes potentially usable organic materials almost uncountable<sup>[83]</sup>. These functional organic materials can not only expand the interlayer spacing but also offset the intrinsic drawback. For example, the electronic conductivity of  $\text{NH}_4\text{V}_3\text{O}_8$  was improved when a conductive polymer, poly(3,4-ethylenedioxythiophene), was inserted<sup>[84]</sup>.

## 4. Conclusions and outlook

In the post-LIB era, PIBs have aroused wide attention by virtue of their similar electrochemical properties to those of LIBs and strong economic competitiveness. Nonetheless, the relative research is still in its infancy, and many issues remain to be further explored. The development of electrode materials is certainly of critical importance. The vanadium oxide family includes cathode and anode materials, some of which can be used as both. Vanadium is a rock-forming and earth-abundant element, which meets the demand for low-cost and large-scale production. Its multivalent properties provide more possibilities for structural, material, and physicochemical properties. Serving as PIB electrode materials, they are mainly restricted by their low electronic conductivity and large volume expansion. These problems can be solved or alleviated to some extent using appropriate methods, such as carbon material coating, morphology design, defect engineering and heteroatom doping, and interlayer expansion, as discussed in Section 3. Meanwhile, these strategies can improve the electrochemical performance. At present, although encouraging research results have been achieved, there are still many challenges to be solved and much room for improvement. By summarizing the recent research progress, we believe that the following points may be possible research directions.

(1) Exploring other vanadium oxides. Actually, there are a large number of members in the vanadium oxide family, and many of them exhibited superior electrochemical performance in various battery systems such as lithium-, sodium-calcium-, and zinc-ion batteries<sup>[48]</sup>. However, until now, only a few vanadium oxides have been employed as electrode materials for PIBs. In this case, it is necessary to investigate the K storage capability of those vanadium oxides that have not been used in PIBs or develop novel vanadium oxides. Metal-ion intercalated vanadium oxides, such as alkali metal ions (e.g.  $\text{Li}^+$ ,  $\text{Na}^+$ , and  $\text{K}^+$ ), alkali earth metal ions (e.g.  $\text{Ca}^{2+}$ ,  $\text{Mg}^{2+}$ , and  $\text{Sr}^{2+}$ ), and transition metal ions (e.g.  $\text{Co}^{2+}$ ,  $\text{Cu}^{2+}$ , and  $\text{Zn}^{2+}$ ), are worth being given more attention because of their material and electrochemical properties.

(2) Reasonable material design. As mentioned earlier, many strategies can solve the problems faced by vanadium oxides, and improve their material stability and electrochemical performance. Sometimes, positive effects may be achieved when they are used in a synergistic manner. Taking carbon material coating as an example, it can not only improve the electronic conductivity but also buffer the volume expansion. Nonetheless, the practical application of electrode materials should be considered in such a commercialization-oriented research field. For instance, carbon material coating is a “double-edged sword” because the low tapping density of carbon materials results in a low volumetric energy density of batteries. Therefore, researchers should balance the positive and negative effects derived from the above-mentioned improvement strategies during electrode material design.

(3) Electrochemical reaction mechanisms. In the reported works, the study on the electrochemical reaction mechanism of vanadium oxides is not clear and detailed. Many analyses are reasonable inferences based on the results obtained from LIBs or SIBs. However, the discrepancies of alkali metal ions may lead to significantly different charge storage mechanisms regardless of the physical and chemical similarities<sup>[27, 85]</sup>. In this regard, the electrochemical reaction mechanism should be further studied. Emerging in situ/operando characterizations that can directly and timely monitor continuous electrochemical reaction processes are reliable and powerful techniques to elucidate electrochemical reaction mechanisms<sup>[86]</sup>. In addition, computational simulation is also an important tool and can provide a corresponding theoretical basis.

All in all, despite the many challenges, the obtained inspiring research results and superior intrinsic properties make vanadium oxides become promising electrode materials for PIBs. We hope that our review has provided valuable information to facilitate the development of this kind of material.

## Acknowledgements

This work was supported by the Shenyang University of Technology (QNPY202209-4), the Key R&D project of Liaoning Province of China (2020JH2/10300079), the “Liaoning BaiQi-anWan Talents Program” (2018921006), the Liaoning Revitalization Talents Program (XLYC1908034), and the National Natural Science Foundation of China (21571132).

## References

- [1] Zhou M, Xu Y, Lei Y. Heterogeneous nanostructure array for electrochemical energy conversion and storage. *Nano Today*, 2018, 20, 33
- [2] Xu R, Du L, Adekoya D, et al. Well-defined nanostructures for electrochemical energy conversion and storage. *Adv Energy Mater*, 2020, 11, 2001537
- [3] Xu Y, Zhou M, Lei Y. Nanoarchitected array electrodes for rechargeable lithium- and sodium-ion batteries. *Adv Energy Mater*, 2016, 6, 1502514
- [4] Wu J, Hong Y and Wang B. The applications of carbon nanomaterials in fiber-shaped energy storage devices. *J Semicond*, 2018, 39, 011004
- [5] Guo Y, Zhang Y, Lu H. Manganese-based materials as cathode for rechargeable aqueous zinc-ion batteries. *Battery Energy*, 2022, 1, 20210014
- [6] Zhu Y, Xiao Y, Dou S, et al. Spinel/Post-spinel engineering on

- layered oxide cathodes for sodium-ion batteries. *eScience*, 2021, 1, 13
- [7] Hang W, Qi Y, Nan Z, et al. Roadmap of amorphous metal-organic framework for electrochemical energy conversion and storage. *Nano Res*, 2022
- [8] Zhu H, Sha M, Zhao H, et al. Highly-rough surface carbon nanofibers film as an effective interlayer for lithium-sulfur batteries. *J Semicond*, 2020, 41, 092701
- [9] Nasori N, Dai T, Jia X, et al. Realizing super-long  $\text{Cu}_2\text{O}$  nanowires arrays for high-efficient water splitting applications with a convenient approach. *J Semicond*, 2019, 40, 052701
- [10] Liu J, Wang Z, Lei Y. A close step towards industrialized application of solar water splitting. *J Semicond*, 2020, 41, 090401
- [11] Zhao C, Wang Z, Shu D, et al. Preface to the special issue on challenges and possibilities of energy storage. *J Semicond*, 2020, 41, 090101
- [12] Yang S, Zhang F, Ding H, et al. Lithium metal extraction from seawater. *Joule*, 2018, 2, 1648
- [13] Wu Y, Zhang C, Zhao H, et al. Recent advances in ferromagnetic metal sulfides and selenides as anodes for sodium- and potassium-ion batteries. *J Mater Chem A*, 2021, 9, 9506
- [14] Sigma-Aldrich. <https://www.sigmaaldrich.com>
- [15] Xu Y S, Duan S Y, Sun Y G, et al. Recent developments in electrode materials for potassium-ion batteries. *J Mater Chem A*, 2019, 7, 4334
- [16] Hosaka T, Kubota K, Hameed A S, et al. Research development on K-ion batteries. *Chem Rev*, 2020, 120, 6358
- [17] Kim H, Kim J C, Bianchini M, et al. Recent progress and perspective in electrode materials for K-ion batteries. *Adv Energy Mater*, 2017, 8, 1702384
- [18] Pramudita J C, Sehwat D, Goonetilleke D, et al. An initial review of the status of electrode materials for potassium-ion batteries. *Adv Energy Mater*, 2017, 7, 1602911
- [19] Kubota K, Dahbi M, Hosaka T, et al. Towards K-ion and Na-ion batteries as "beyond Li-ion". *Chem Rec*, 2018, 18, 459
- [20] Yabuuchi N, Kubota K, Dahbi M, et al. Research development on sodium-ion batteries. *Chem Rev*, 2014, 114, 11636
- [21] Wu Y, Wu X, Guan Y, et al. Carbon-based flexible electrodes for electrochemical potassium storage devices. *New Carbon Mater*, 2022, 37, 852
- [22] Wu X, Leonard DP, Ji X. Emerging non-aqueous potassium-ion batteries: Challenges and opportunities. *Chem Mater*, 2017, 29, 5031
- [23] Xu Y, Zhang C, Zhou M, et al. Highly nitrogen doped carbon nanofibers with superior rate capability and cyclability for potassium ion batteries. *Nat Commun*, 2018, 9, 1720
- [24] Jian Z, Luo W, Ji X. Carbon electrodes for K-ion batteries. *J Am Chem Soc*, 2015, 137, 11566
- [25] Wu Y, Zhang Q, Xu Y, et al. Enhanced potassium storage capability of two-dimensional transition-metal chalcogenides enabled by a collective strategy. *ACS Appl Mater Interfaces*, 2021, 13, 18838
- [26] Wu Y, Xu R, Wang Z, et al. Carbon-free crystal-like  $\text{Fe}_{1-x}\text{S}$  as an anode for potassium-ion batteries. *ACS Appl Mater Interfaces*, 2021, 13, 55218
- [27] Wu Y, Xu Y, Li Y, et al. Unexpected intercalation-dominated potassium storage in  $\text{WS}_2$  as a potassium-ion battery anode. *Nano Res*, 2019, 12, 2997
- [28] Lei K, Wang C, Liu L, et al. A porous network of bismuth used as the anode material for high-energy-density potassium-ion batteries. *Angew Chem Int Ed*, 2018, 57, 4687
- [29] Liu Q, Fan L, Ma R, et al. Super long-life potassium-ion batteries based on an antimony@carbon composite anode. *Chem Commun*, 2018, 54, 11773
- [30] Liang Y, Luo C, Wang F, et al. An organic anode for high temperature potassium-ion batteries. *Adv Energy Mater*, 2018, 9, 1802986
- [31] Ma J, Zhou E, Fan C, et al. Endowing CuTCNQ with a new role: a high-capacity cathode for K-ion batteries. *Chem Commun*, 2018, 54, 5578
- [32] Chen M, Liu Q, Hu Z, et al. Designing advanced vanadium-based materials to achieve electrochemically active multielectron reactions in sodium/potassium-ion batteries. *Adv Energy Mater*, 2020, 10, 2002244
- [33] Wang Q, Xu J, Zhang W, et al. Research progress on vanadium-based cathode materials for sodium ion batteries. *J Mater Chem A*, 2018, 6, 8815
- [34] Esparcia E, Joo J, Lee J. Vanadium oxide bronzes as cathode active materials for non-lithium-based batteries. *CrystEngComm*, 2021, 23, 5267
- [35] Luo W, Gaumet J J, Mai L. Nanostructured layered vanadium oxide as cathode for high-performance sodium-ion batteries: A perspective. *MRS Commun*, 2017, 7, 152
- [36] Koch D, Kulish V V, Manzhos S. A first-principles study of potassium insertion in crystalline vanadium oxide phases as possible potassium-ion battery cathode materials. *MRS Commun*, 2017, 7, 819
- [37] Baddour-Hadjean R, Safrany Renard M, Pereira-Ramos J P. Unraveling the structural mechanism of Li insertion in  $\gamma\text{-V}_2\text{O}_5$  and its effect on cycling properties. *Acta Mater*, 2019, 165, 183
- [38] Safrany Renard M, Emery N, Baddour-Hadjean R, et al.  $\gamma\text{-V}_2\text{O}_5$ : A new high voltage cathode material for sodium-ion battery. *Electrochim Acta*, 2017, 252, 4
- [39] Muller-Bouvet D, Baddour-Hadjean R, Tanabe M, et al. Electrochemically formed  $\alpha\text{-NaV}_2\text{O}_5$ : A new sodium intercalation compound. *Electrochim Acta*, 2015, 176, 586
- [40] Baddour-Hadjean R, Safrany Renard M, Emery N, et al. The richness of  $\text{V}_2\text{O}_5$  polymorphs as superior cathode materials for sodium insertion. *Electrochim Acta*, 2018, 270, 129
- [41] Bhatia A, Pereira-Ramos J P, Emery N, et al.  $\gamma\text{-V}_2\text{O}_5$  Polymorph as a promising host structure for potassium storage: an electrochemical and structural study. *Chem Mater*, 2021, 33, 5276
- [42] Tian B, Tang W, Su C, et al. Reticular  $\text{V}_2\text{O}_5\cdot 0.6\text{H}_2\text{O}$  xerogel as cathode for rechargeable potassium ion batteries. *ACS Appl Mater Interfaces*, 2018, 10, 642
- [43] Ye F, Lu D, Gui X, et al. Atomic layer deposition of core-shell structured  $\text{V}_2\text{O}_5$ @CNT sponge as cathode for potassium ion batteries. *J Materiomics*, 2019, 5, 344
- [44] Vishnuprakash P, Nithya C, Premalatha M. Exploration of  $\text{V}_2\text{O}_5$  nanorod@rGO heterostructure as potential cathode material for potassium-ion batteries. *Electrochim Acta*, 2019, 309, 234
- [45] Tian Y, An Y, Wei H, et al. Micron-sized nanoporous vanadium pentoxide arrays for high-performance gel zinc-ion batteries and potassium batteries. *Chem Mater*, 2020, 32, 4054
- [46] Jiang X, Tian S, Jiang Q, et al. A  $\text{V}_2\text{O}_5$ -based freestanding anode with high rate and superior cycle life for potassium storage. *Comp Comm*, 2022, 32, 101172
- [47] Wei M D, Sugihara H, Honma I, et al. A new metastable phase of crystallized  $\text{V}_2\text{O}_4\cdot 0.25\text{H}_2\text{O}$  nanowires: Synthesis and electrochemical measurements. *Adv Mater*, 2005, 17, 2964
- [48] Xu X, Xiong F, Meng J, et al. Vanadium-based nanomaterials: A promising family for emerging metal-ion batteries. *Adv Funct Mater*, 2020, 30, 1904398
- [49] Chernova N A, Roppolo M, Dillon A C, et al. Layered vanadium and molybdenum oxides: batteries and electrochromics. *J Mater Chem*, 2009, 19, 2526
- [50] Wu C, Xie Y. Promising vanadium oxide and hydroxide nanostructures: from energy storage to energy saving. *Energy Environ Sci*, 2010, 3, 1191
- [51] Li Y, Zhang Q, Yuan Y, et al. Surface amorphization of vanadium dioxide (B) for K-ion battery. *Adv Energy Mater*, 2020, 10, 2000717
- [52] Jin D, Gao Y, Zhang D, et al.  $\text{VO}_2$ @Carbon foam as a freestanding anode material for potassium-ion batteries: First principles and ex-

- perimental study. *J Alloys Compd*, 2020, 845, 156232
- [53] Chen F, Wang S, He X D, et al. Hollow sphere structured  $V_2O_3@C$  as an anode material for high capacity potassium-ion batteries. *J Mater Chem A*, 2020, 8, 13261
- [54] Chen J, Wang T, Chen C, et al. Heteroatom doping hollow vanadium oxide/carbon composites as universal anode materials for efficient alkali-metal ion storage. *Carbon*, 2022, 192, 30
- [55] Tong Z, Yang R, Wu S, et al. Defect-engineered vanadium trioxide nanofiber bundle@graphene hybrids for high-performance all-vanadate Na-ion and K-ion full batteries. *J Mater Chem A*, 2019, 7, 19581
- [56] Zhao Y, Han C, Yang J, et al. Stable alkali metal ion intercalation compounds as optimized metal oxide nanowire cathodes for lithium batteries. *Nano Lett*, 2015, 15, 2180
- [57] Clites M, Hart J L, Taheri M L, et al. Chemically preintercalated bilayered  $K_xV_2O_5 \cdot nH_2O$  nanobelts as a high-performing cathode material for K-ion batteries. *ACS Energy Lett*, 2018, 3, 562
- [58] Zhu Y H, Zhang Q, Yang X, et al. Reconstructed orthorhombic  $V_2O_5$  polyhedra for fast ion diffusion in K-ion batteries. *Chem*, 2019, 5, 168
- [59] Liang G, Gan Z, Wang X, et al. Reconstructing vanadium oxide with anisotropic pathways for a durable and fast aqueous K-ion battery. *ACS Nano*, 2021, 15, 17717
- [60] Zhang Y, Niu X, Tan L, et al.  $K_{0.83}V_2O_5$ : A new layered compound as a stable cathode material for potassium-ion batteries. *ACS Appl Mater Interfaces*, 2020, 12, 9332
- [61] Li X, Zhuang C, Xu J, et al. Rational construction of  $K_{0.5}V_2O_5$  nanobelts/CNTs flexible cathode for multi-functional potassium-ion batteries. *Nanoscale*, 2021, 13, 8199
- [62] Deng Q, Zhao Z, Wang Y, et al. A stabilized polyacrylonitrile-encapsulated matrix on a nanolayered vanadium-based cathode material facilitating the K-storage performance. *ACS Appl Mater Interfaces*, 2022, 14, 14243
- [63] Niu X, Qu J, Hong Y, et al. High-performance layered potassium vanadium oxide for K-ion batteries enabled by reduced long-range structural order. *J Mater Chem A*, 2021, 9, 13125
- [64] Liu C, Luo S, Huang H, et al. Potassium vanadate  $K_{0.23}V_2O_5$  as anode materials for lithium-ion and potassium-ion batteries. *J Power Sources*, 2018, 389, 77
- [65] Lu M, Wang K F, Ke H D, et al. Potassium vanadate  $K_2V_3O_8$  as a superior anode material for potassium-ion batteries. *Mater Lett*, 2018, 232, 224
- [66] Jo J H, Hwang J Y, Choi J U, et al. Potassium vanadate as a new cathode material for potassium-ion batteries. *J Power Sources*, 2019, 432, 24
- [67] Yang Y, Liu Z, Deng L, et al. A non-topotactic redox reaction enabled  $K_2V_3O_8$  as a high voltage cathode material for potassium-ion batteries. *Chem Commun*, 2019, 55, 14988
- [68] Charles D S, Feygenson M, Page K, et al. Structural water engaged disordered vanadium oxide nanosheets for high capacity aqueous potassium-ion storage. *Nat Commun*, 2017, 8, 15520
- [69] Xu Y, Dong H, Zhou M, et al. Ammonium vanadium bronze as a potassium-ion battery cathode with high rate capability and cyclability. *Small Methods*, 2019, 3, 1800349
- [70] Rastgoo-Deylami M, Heo J W, Hong S T. High potassium storage capability of  $H_2V_3O_8$  in a non-aqueous electrolyte. *ChemistrySelect*, 2019, 4, 11711
- [71] Lu J, Wang C, Xia G, et al. A robust spring-like lamellar VO/C nanostructure for high-rate and long-life potassium-ion batteries. *J Mater Chem A*, 2020, 8, 23939
- [72] Liu T, Li L, Yao T, et al. Integrating amorphous vanadium oxide into carbon nanofibers via electrospinning as high-performance anodes for alkaline ion ( $Li^+/Na^+/K^+$ ) batteries. *Electrochim Acta*, 2021, 369, 137711
- [73] Kuai X, Li K, Chen J, et al. Interfacial engineered vanadium oxide nanoheterostructures synchronizing high-energy and long-term potassium-ion storage. *ACS Nano*, 2022, 16, 1502
- [74] Ouyang D, Wang C, Yang L, et al. Enhancing potassium storage performance in  $VO_2/V_2O_3@C$  nanosheets by synergistic effect of oxygen vacancy and C-O-V bond. *ChemElectroChem*, 2022, 9, 202200639
- [75] Ren X, Ai D, Zhan C, et al. NaCl-template-assisted freeze-drying synthesis of 3D porous carbon-encapsulated  $V_2O_3$  for lithium-ion battery anode. *Electrochim Acta*, 2019, 318, 730
- [76] Yang G, Wu Y, Fu Q, et al. Nanostructured metal selenides as anodes for potassium-ion batteries. *Sustain Energy Fuels*, 2022, 6, 2087
- [77] Hu Z, Liu Q, Chou S L, et al. Advances and challenges in metal sulfides/selenides for next-generation rechargeable sodium-ion batteries. *Adv Mater*, 2017, 29, 1700606
- [78] Zhu K, Wei S, Shou H, et al. Defect engineering on  $V_2O_3$  cathode for long-cycling aqueous zinc metal batteries. *Nat Commun*, 2021, 12, 6878
- [79] Ren Q, Qin N, Liu B, et al. An oxygen-deficient vanadium oxide@N-doped carbon heterostructure for sodium-ion batteries: insights into the charge storage mechanism and enhanced reaction kinetics. *J Mater Chem A*, 2020, 8, 3450
- [80] Hu B, Li L, Xiong X, et al. High-performance of copper-doped vanadium pentoxide porous thin films cathode for lithium-ion batteries. *J Solid State Electrochem*, 2019, 23, 1315
- [81] Wu F, Wang Y, Ruan P, et al. Fe-doping enabled a stable vanadium oxide cathode with rapid Zn diffusion channel for aqueous zinc-ion batteries. *Mater Today Energy*, 2021, 21, 100842
- [82] Ghosh M, Dilwale S, Vijayakumar V, et al. Scalable synthesis of manganese-doped hydrated vanadium oxide as a cathode material for aqueous zinc-metal battery. *ACS Appl Mater Interfaces*, 2020, 12, 48542
- [83] Xiong P, Wu Y, Liu Y, et al. Two-dimensional organic-inorganic superlattice-like heterostructures for energy storage applications. *Energy Environ Sci*, 2020, 13, 4834
- [84] Bin D, Huo W, Yuan Y, et al. Organic-inorganic-induced polymer intercalation into layered composites for aqueous zinc-ion battery. *Chem*, 2020, 6, 968
- [85] Lin H, Li M, Yang X, et al. Nanosheets-assembled CuSe crystal pillar as a stable and high-power anode for sodium-ion and potassium-ion batteries. *Adv Energy Mater*, 2019, 9, 1900323
- [86] Liu D, Shadik Z, Lin R, et al. Review of recent development of in situ/operando characterization techniques for lithium battery research. *Adv Mater*, 2019, 31, 1806620



**Yuhan Wu** received his Ph.D. degree in material physics at the Ilmenau University of Technology in 2021. Since 2022, he has been a lecturer at the Shenyang University of Technology. His research interests focus on designing and synthesizing nanostructural materials for energy conversion and storage.



**Yinyan Guan** got her B.S. degree in 2007 at the Beijing University of Chemical Technology and Ph.D. degree in 2014 at the Institute of Chemistry, Chinese Academy of Sciences. Then she joined the Shenyang University of Technology as an associate professor. Her research interests include polymer processing, polymer membranes, and thin film batteries.



**Juan Hou** got her B.S. degree in 2006 and Ph.D. degree in 2013 at the University of Chinese Academy of Sciences. She is currently a professor at Shihezi University. Her research interests are new energy materials and devices.



**Fanian Shi** received his Ph.D. in applied chemistry in 1996 at Changchun Institute of Applied Chemistry, Chinese Academy of Sciences. He is currently a full professor at the Shenyang University of Technology and a member of the committee on Energy and Environment, China Energy Society. He specializes in the research of MOF composites for energy materials, photocatalysts, etc.